

## Original Article

## Nanoparticle delivery of chemotherapy combination regimen improves the therapeutic efficacy in mouse models of lung cancer



Jing Tian, PhD<sup>a,b,c,1</sup>, Yuangzeng Min, PhD<sup>b,c,1</sup>, Zachary Rodgers, PhD<sup>b,c</sup>, Xiaomeng Wan, B.S.<sup>d</sup>, Hui Qiu, M.S.<sup>b,c,e</sup>, Yu Mi, PhD<sup>b,c</sup>, Xi Tian, PhD<sup>b,c</sup>, Kyle T. Wagner, B.S.<sup>b,c</sup>, Joseph M. Caster, MD, PhD<sup>b,c</sup>, Yanfei Qi, PhD<sup>b,c,h</sup>, Kyle Roche, PhD<sup>b,c</sup>, Tian Zhang, MD<sup>f</sup>, Jianjun Cheng, PhD<sup>g</sup>, Andrew Z. Wang, MD<sup>b,c,\*</sup>

<sup>a</sup> School of Biological and Environmental Engineering, Tianjin Vocational Institute, Tianjin, PR China

<sup>b</sup> Laboratory of Nano- and Translational Medicine, Lineberger Comprehensive Cancer Center, Carolina Center for Cancer Nanotechnology Excellence, Carolina Institute of Nanomedicine, University of North Carolina at Chapel Hill, Chapel Hill, NC, USA

<sup>c</sup> Department of Radiation Oncology, Lineberger Comprehensive Cancer Center, University of North Carolina at Chapel Hill, Chapel Hill, NC, USA

<sup>d</sup> Division of Molecular Pharmaceutics, Center for Nanotechnology in Drug Delivery, Eshelman School of Pharmacy, University of North Carolina at Chapel Hill, Chapel Hill, NC, USA

<sup>e</sup> Department of Radiation Oncology, Affiliated Hospital of Xuzhou Medical University, Xuzhou, China

<sup>f</sup> Division of Medical Oncology, Department of Medicine, Duke University Medical Center, Durham, NC, USA

<sup>g</sup> Department of Materials Science and Engineering, University of Illinois at Urbana-Champaign, Urbana, IL, USA

<sup>h</sup> School of Public Health, Jilin University, Changchun, Jilin, China

## ARTICLE INFO

## Article history:

Received 8 August 2016

Accepted 17 November 2016

## Key words:

Drug delivery

PLGA-PEG

Cisplatin prodrugs

Docetaxel

Combination therapy

## ABSTRACT

The combination chemotherapy regimen of cisplatin (CP) and docetaxel (DTX) is effective against a variety of cancers. However, combination therapies present unique challenges that can complicate clinical application, such as increases in toxicity and imprecise exposure of tumors to specific drug ratios that can produce treatment resistance. Drug co-encapsulation within a single nanoparticle (NP) formulation can overcome these challenges and further improve combinations' therapeutic index. In this report, we employ a CP prodrug (CPP) strategy to formulate poly(lactic-co-glycolic acid)-poly(ethylene glycol) (PLGA-PEG) NPs carrying both CPP and DTX. The dually loaded NPs display differences in drug release kinetics and *in vitro* cytotoxicity based on the structure of the chosen CPP. Furthermore, NPs containing both drugs showed a significant improvement in treatment efficacy versus the free drug combination *in vivo*.

© 2016 Elsevier Inc. All rights reserved.

**Abbreviations:** AST, aspartate aminotransferase; ALT, alanine aminotransferase; BUN, blood urea nitrogen; C<sub>4</sub>CP, butyrate modified Pt(IV); C<sub>8</sub>CP, octanoate modified Pt(IV); C<sub>10</sub>CP, decanoate modified Pt(IV); CP, cisplatin; CPP, cisplatin prodrug; Crea, creatine; DPBS, Dulbecco's® phosphate buffered saline; DTX, docetaxel; %EE, encapsulation efficiency; %FR, feeding ratio; MTS, 3-(4,5-dimethylthiazol-2-yl)-5-(3-carboxymethoxyphenyl)-2-(4-sulfophenyl)-2H-tetrazolium; NP, nanoparticle; PLGA-PEG, poly(lactic-co-glycolic acid)-poly(ethylene glycol).

This work was supported by National Institutes of Health/National Cancer Institute (R01CA178748-01) and National Institutes of Health/National Cancer Institute (U54CA198999, Carolina Center of Cancer Nanotechnology Excellence (CCNE)-Nano Approaches to Modulate Host Cell Response for Cancer Therapy). Jing Tian is supported by the Natural Science Foundation of Tianjin (Grant No. 15JCYBJC21100) and the Science & Technology Development Fund of Tianjin Education Commission for Higher Education (No. 20110511). Zachary Rodgers is supported by the Carolina Cancer Nanotechnology T32 Training Program (C-CNTP, NIH-1T32CA196589). Andrew Wang was also supported by funding from the NIH/NCI (R21 CA182322).

The authors report no conflict of interests.

\* Corresponding author at: Department of Radiation Oncology, Lineberger Comprehensive Cancer Center, University of North Carolina at Chapel Hill, Chapel Hill, NC 27599, USA.

E-mail address: [zawang@med.unc.edu](mailto:zawang@med.unc.edu) (A.Z. Wang).

<sup>1</sup> These authors contributed equally to this work.

Despite recent advances in molecularly targeted therapies and immunotherapies, cytotoxic chemotherapy regimens remain the most effective option in the management of cancers. Chemotherapeutics are commonly given in combination to overcome treatment resistance and to take advantage of synergistic effects that allow one drug to improve the therapeutic index of another.<sup>1–3</sup> However, combination chemotherapy presents its own clinical challenges, such as leading to increases in toxicity. Moreover, due to the differences in drugs' physico-chemical and pharmacokinetic properties, many tumor cells are not equally exposed to both chemotherapeutics in the desired ratio and dosage, leading to treatment resistance.<sup>2,4–7</sup> The recent clinical success of a liposomal formulation containing cytarabine and daunorubicin suggests that co-delivery of chemotherapeutics *via* NP carriers can overcome treatment resistance, reduce systemic side effects, and further improve a combination's therapeutic efficacy.<sup>8,9</sup> Yet, to achieve the maximum therapeutic efficacy, many key challenges remain in the development of combination nanotherapeutics, such as delivering drugs that have very different chemical properties at a precise ratio and in a temporal manner.

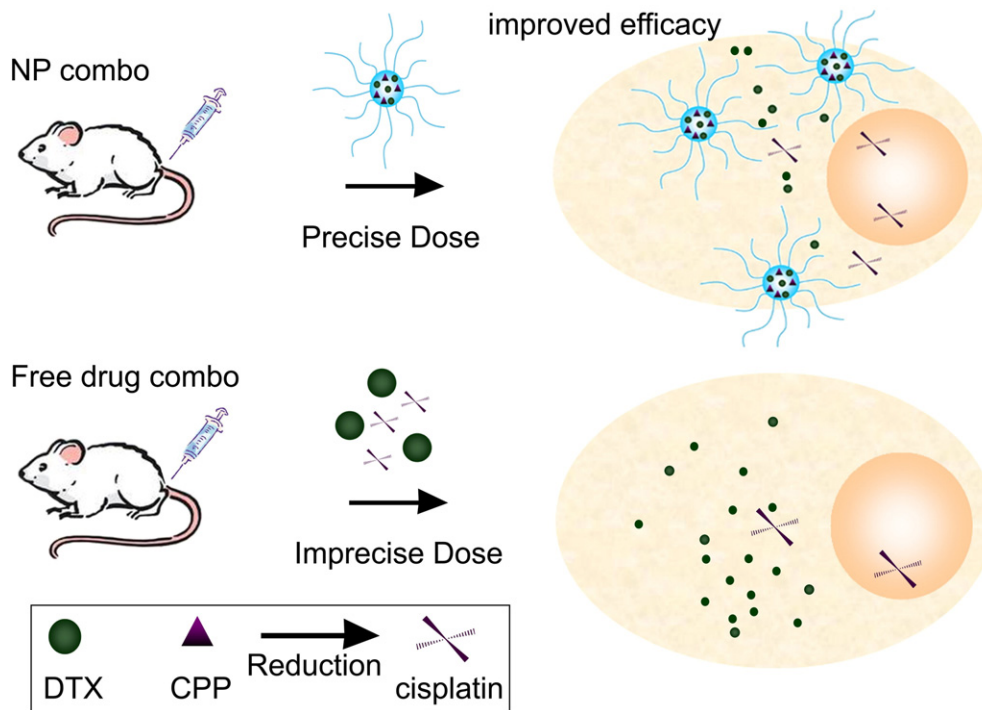


**Figure 1.** CPP and DTX co-delivery from PLGA–PEG NPs. NP co-encapsulation allows for accurate exposure of the murine tumor site to both drugs whereas freely dosed drugs may lead to variations in tumor-drug exposure and reductions in potency.

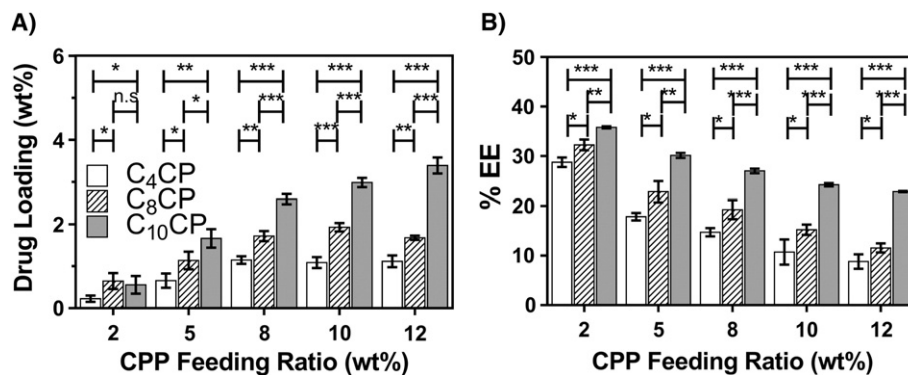


**Figure 2.** (A) Drug loading (wt%) and (B) encapsulation efficiency (%EE) of the singly drug-loaded C<sub>4</sub>CP, C<sub>8</sub>CP, and C<sub>10</sub>CP NPs. PLGA–PEG NPs were formed by nanoprecipitation in the presence of CPPs at different %FR. After NP formation and washing, final drug loadings were determined using digestion followed by HPLC analysis. n.s. indicates no significant difference; \* indicates  $P < 0.05$ ; \*\* indicates  $P < 0.01$ ; \*\*\* indicates  $P < 0.001$ .

In this report, we aimed to address these challenges by developing an NP combination formulation of DTX and CP; a commonly utilized chemotherapy regimen effective against lung, gastric, and head and neck cancers.<sup>10–16</sup> As proof-of-principle, we utilized poly(lactic acid-co-glycolic acid)–poly(ethylene glycol) (PLGA–PEG) NPs for our study, since this system is a proven and well-tolerated platform for drug delivery applications.<sup>17</sup> However, hydrophilic CP loads poorly within the hydrophobic core of PLGA–PEG NPs, so we employed a proven cisplatin prodrug (CPP) strategy that increases the CP's hydrophobic character by modifying an oxidized precursor platinum(IV) complex with fatty acid chains (Figures 1 and S1).<sup>18–20</sup> The fatty acid modifications increase the complex's hydrophobicity and promotes CPP co-encapsulation with DTX in similarly hydrophobic PLGA–PEG NPs. The fatty acid modified CPPs can form free CP after intracellular reduction generates the active Pt(II) square planar complex (Figure S1).

In this work, we examined several formulations of DTX and CPPs with varying hydrophobicities for differences in drug release kinetics

and ideal dosing ratios when co-encapsulated within PLGA–PEG NPs. Furthermore, we evaluated the *in vitro* and *in vivo* efficacies of these NP formulations using lung cancer as a model disease

## Methods

Additional synthesis and characterization details are available in the supplementary information.

## Cell culture

The lung cancer cell line, H460, was obtained from American Type Culture Collection (ATCC) supplied by the Tissue Culture Facility at the UNC Lineberger Comprehensive Cancer Center. The 344SQ cell line was a generous gift from Professor Chad Pecot's lab. Cells were cultured in RPMI-1640 medium supplemented with fetal bovine serum (10% v/v)

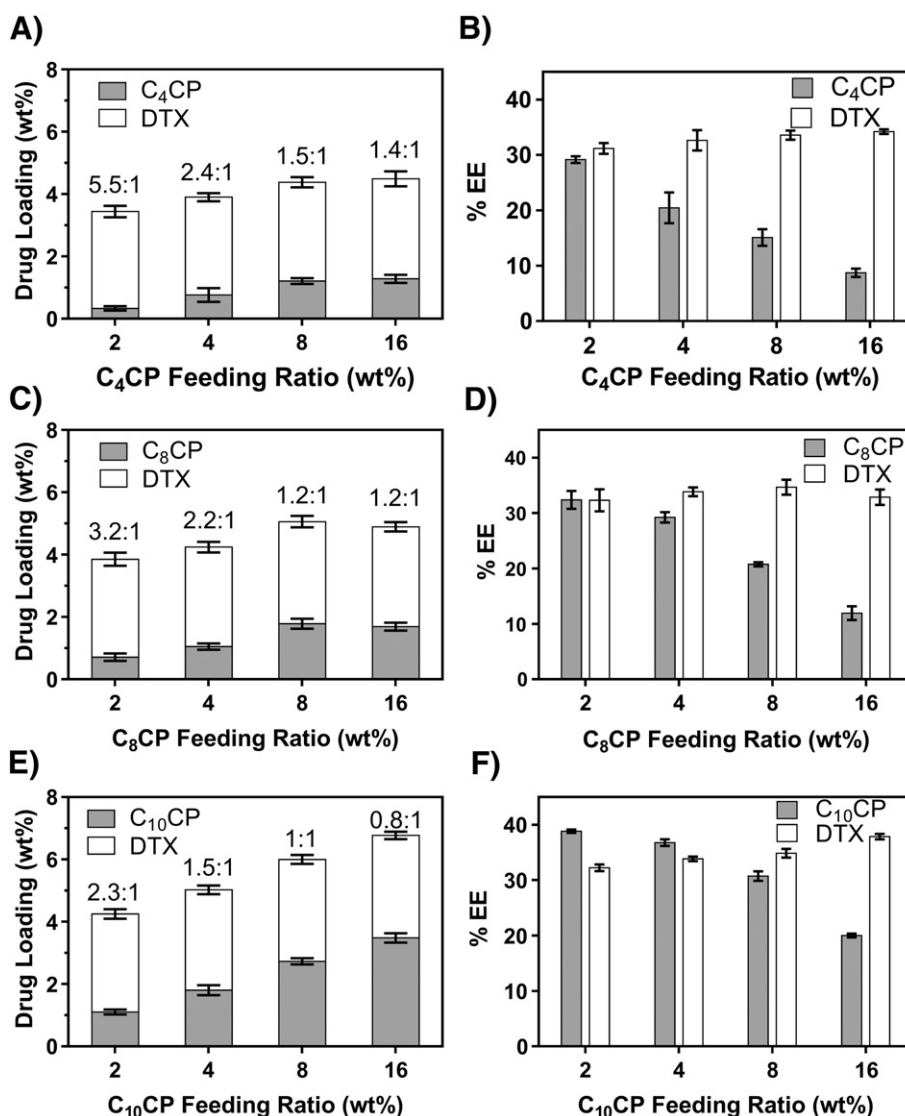


**Figure 3.** Drug loading (wt%) and encapsulation efficiency (% EE) of dually loaded NPs. PLGA–PEG NPs were formed with a constant 10%FR DTX and various %FR of (A, B) C<sub>4</sub>CP, (C, D) C<sub>8</sub>CP, or (E, F) C<sub>10</sub>CP. The ratios shown above each bar in panels A, C, and E correspond to the DTX:CPP molar ratio encapsulated in the NPs.

and penicillin/streptomycin for the H460 (1% v/v) or puromycin for 344SQ (4 μg/mL).

#### Animal maintenance

Six to eight week old, female, athymic nude mice weighing 20–30 g were supplied by the University of North Carolina animal facility and maintained under pathogen-free conditions in the Center for Experimental Animals (an AAALAC accredited experimental animal facility). The animal use protocol was approved by the University of North Carolina Institutional Animal Care and Use committee and conformed to the Guide for the Care and Use of Laboratory Animals (NIH publication no. 86-23, revised 1985).

#### Preparation of PLGA–PEG NPs loaded with different drug ratios

PLGA–PEG was chosen as the NP platform due to its high clinical translation potential.<sup>21</sup> DTX and CPPs were loaded into PLGA NPs via a nanoprecipitation method.<sup>18</sup> Briefly, different feeding ratios (%FR, defined as wt% drug versus polymer) of drugs and PLGA–PEG (5 mg) were dissolved in acetonitrile (200 μL). The drug-polymer solution

was then added drop-wise into deionized water (4 mL) under constant stirring. For singly loaded NPs, the DTX and CPP feeding ratios (%FR) were varied between 2 and 12 wt% (Figures 2 and S2; Table S1). For dually loaded NPs, the DTX %FR was held constant at 10 wt% due to its high encapsulation at this %FR, and the CPPs' %FR was varied between 2 and 16 wt% (Figure 3; Tables S2 and S3). The NP suspension was allowed to stir uncovered for 3 h at room temperature to evaporate the acetonitrile. The resulting NPs were purified by ultra-centrifugation using an Amicon Ultra-4 filter (MWCO: 30 kDa) at 1000g for 15 min (Millipore, Billerica, MA, USA). The PLGA–PEG NPs were washed with deionized water (3×) then suspended in PBS. Final drug loading was determined using high performance liquid chromatography (HPLC, see SI).

#### In vitro release of CPPs and DTX from PLGA–PEG NPs

In vitro drug-release profiles of loaded NPs were recorded under physiological sink conditions (Figure 4).<sup>22</sup> NP solutions (500 μL) were split into Slide-A-Lyzer MINI dialysis microtubes (20 kDa MWCO, Pierce, Rockford, IL, USA) and dialyzed against a large excess of PBS (1 L) with gentle stirring at 37 °C. At the indicated times, 10 μL of solution was removed from the microtube and mixed with acetonitrile (60 μL) to

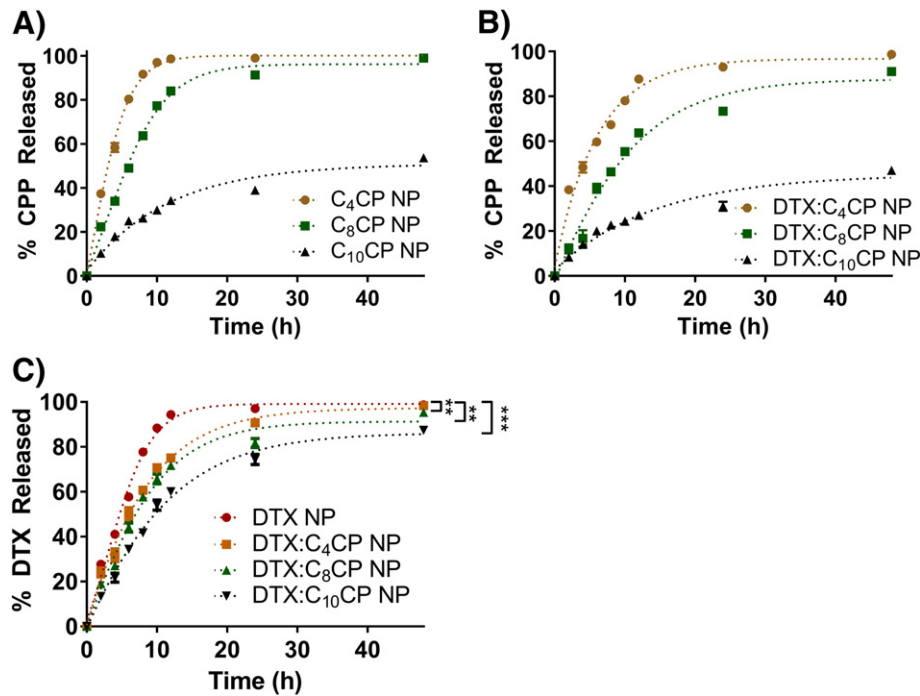


**Figure 4.** Release kinetics of CPPs from (A) singly or (B) dually loaded PLGA–PEG NPs, and (C) DTX release from DTX containing NPs under physiological sink conditions. Loaded NPs were dialyzed against a large excess of PBS and the NPs' retained drug was determined using HPLC after digestion with acetonitrile. \*\* indicates  $P < 0.01$ ; \*\*\* indicates  $P < 0.001$ .

dissolve the NPs. The residual DTX and CPP contents were determined using the HPLC method.

#### *In vitro* cytotoxicity of PLGA–PEG NPs

In a 96-well plate, H460 or 344SQ was plated (5000 cells/well) and allowed to recover overnight. Cells were then dosed with free small-molecule drugs or PLGA–PEG NPs with different drug molar ratios (dosing-1 nM to 20  $\mu$ M). The cells and formulations were incubated in RPMI-1640 complete cell culture medium for 72 h. After incubation, *in vitro* toxicities of the NP drug formulations were evaluated using a 3-(4,5-dimethylthiazol-2-yl)-5-(3-carboxymethoxyphenyl)-2-(4-sulfophenyl)-2H-tetrazolium (MTS) cell viability assay (Promega) (Figure 5; Table S4). IC<sub>50</sub> values were calculated by fitting the dose-dependent cell viabilities to a four-parameter logistic model using the MasterPlex 2010 software pack (MiraiBio Group, Hitachi Solutions America, Ltd.).

#### *In vivo* anticancer efficacy of PLGA–PEG NPs

A murine xenograft tumor model was formed by injecting a suspension of one million (H460) or five million (344SQ) cells (0.1 mL, 50% v/v Matrigel®) into the right flank. Tumors were allowed to grow to a volume 80–150 mm<sup>3</sup> before initiating treatment. Mice were divided into six groups (5–6 mice per group) and treated *via* tail vein injection every 4 days with either (1) PBS (200  $\mu$ L), (2) free CP (1.5 mg/kg) and DTX (3.8 mg/kg), (3) singly loaded mixtures of C<sub>8</sub>CP NPs (2.2 mg/kg) and DTX NPs (3.8 mg/kg), (4) singly loaded mixtures of C<sub>10</sub>CP NPs (2.1 mg/kg) and DTX NPs (3.8 mg/kg), (5) dually loaded C<sub>8</sub>CP (2.2 mg/kg) and DTX (3.8 mg/kg) NPs, or (6) dually loaded C<sub>10</sub>CP (2.1 mg/kg) and DTX (3.8 mg/kg) NPs. Tumor length and width were measured, and the tumor volume was calculated using:  $L \times W^2/2$ , with  $W$  being smaller than  $L$  (Figure 6). Weight and the initial tumor volume were measured and recorded every 2 days. Mice were humanely sacrificed using CO<sub>2</sub> inhalation method when tumor dimensions reached >2 cm in one direction.

#### Toxicity of PLGA–PEG NP formulations

The off-target *in vivo* toxicity of different arms was evaluated in one mouse randomly chosen from each arm 4 days after the last IV injection (Tables S5 and S6). Circulating blood (~1.5 mL) was collected *via* cardiac puncture. For hematological toxicity, 500  $\mu$ L of whole-blood was stored in an EDTA-coated tube at 4 °C and analyzed as previously described for white and red blood cell counts.<sup>22</sup> For hepatotoxicity and nephrotoxicity, whole-blood (1 mL) was transferred to a micro-centrifuge tube and centrifuged (7000 rpm, 5 min) to separate the red blood cells from the plasma. The isolated plasma was analyzed for serum aspartate aminotransferase (AST), alanine aminotransferase (ALT) levels (units/L), blood urea nitrogen (BUN), and creatine (Crea) as previously described.<sup>22</sup>

#### Statistical analysis

All experiments were performed at least three times ( $n = 3$ ), and expressed as mean  $\pm$  SD for *in vitro* or mean  $\pm$  SEM for *in vivo* studies. Statistical differences were determined using two-tailed Student's *t*-test. The significance level was taken as 95% ( $P < 0.05$ ).

## Results

#### Loading characterization of singly and dually drug loaded PLGA–PEG NPs

We prepared three different CPPs modified with butyric (C<sub>4</sub>CP), octanoic (C<sub>8</sub>CP), or decanoic (C<sub>10</sub>CP) fatty acids as previously described (Figure 1).<sup>18,20,23</sup> We determined the drug loading wt% and encapsulation efficiency (%EE) in the NP formulations over a range of tested %FR for all three CPPs and DTX (Figures 2 and S2; Table S1). For singly loaded NPs, the maximal amount of drug loading was found to be  $1.15 \pm 0.09$  wt% ( $14.73 \pm 0.83\%$ EE),  $1.93 \pm 0.10$  wt% ( $15.23 \pm 1.04\%$ EE),  $3.39 \pm 0.19$  wt% ( $22.83 \pm 0.14\%$ EE), and  $3.50 \pm 0.09$  wt% ( $28.65 \pm 1.03\%$ EE) for the C<sub>4</sub>CP (8%FR), C<sub>8</sub>CP (10%FR), C<sub>10</sub>CP (12%FR), and DTX (12%FR), respectively (Table S1). At all %FR greater than 2%, longer fatty acid chains provided greater CP loading values (C<sub>4</sub>CP < C<sub>8</sub>CP < C<sub>10</sub>CP).<sup>20</sup>

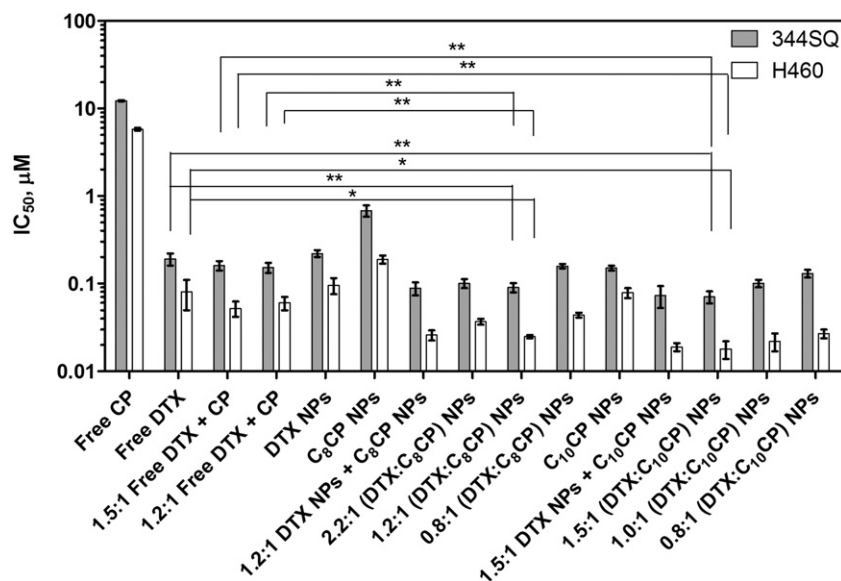


**Figure 5.** *In vitro* cytotoxicity  $IC_{50}$  values of free and encapsulated small molecule chemotherapeutics in a non-small cell (H460) and small cell lung cancer (344SQ) line. Cells were treated with either free drugs, free drugs in combination, singly loaded NPs, singly loaded NPs in combination (DTX NPs + CPP NPs), or dually loaded NPs (DTX:CPP NPs). \* indicates  $P < 0.05$ ; \*\* indicates  $P < 0.01$ ; \*\*\* indicates  $P < 0.001$ .

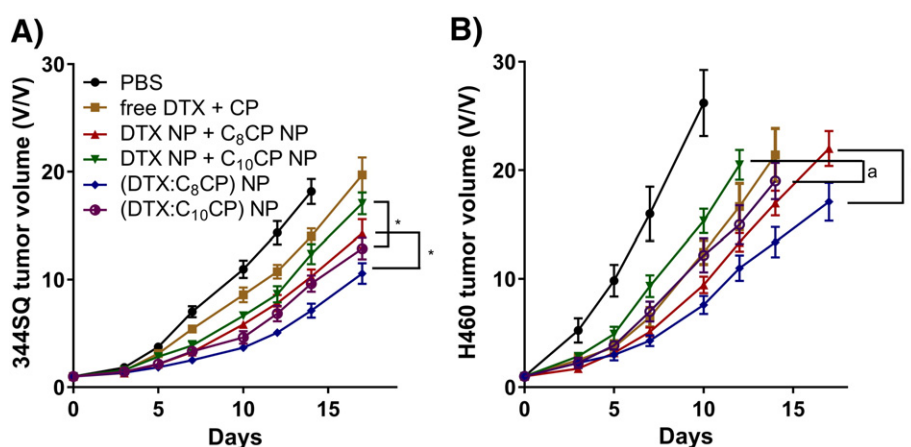


**Figure 6.** Free drug and NP formulation *in vivo* efficacy represented by tumor volume change in (A) 344SQ or (B) H460 murine xenograft models. Mice were treated with combinations of either the free drugs, singly loaded NPs (DTX NP + CPP NP), or dually loaded NPs (DTX:C<sub>8</sub>CP). n.s. indicates no significant difference; \* indicates  $P < 0.05$ , <sup>a</sup> indicates  $P = 0.051$ .

For the dually loaded NPs, the DTX %FR was held constant at 10 wt%. In the presence of DTX, the CPP loading wt% remained consistent with singly loaded NPs. In these combination NPs, the cumulative loading wt% of drugs reached maximum levels of 4.49%, 5.13%, and 6.77% at %FRs of 16 wt% for C<sub>4</sub>CP, 8 wt% for C<sub>8</sub>CP and 16 wt% for C<sub>10</sub>CP, respectively (Figure 3, Table S2). Concurrently, the DTX:CPP molar ratios decreased as the CPPs' %FR increased. Once again, C<sub>10</sub>CP showed the greatest loading ( $3.48 \pm 0.15$  wt%,  $37.86 \pm 0.49\%EE$ ). Due to this higher loading, the C<sub>10</sub>CP shows equivalent NP accumulation versus DTX (1:1) even at a lower 8%FR, whereas more DTX still accumulates within NPs when the C<sub>8</sub>CP is loaded at a much higher 16%FR (1.3:1, DTX:C<sub>8</sub>CP). All three CPPs had minimal effect on DTX loading, since it remained relatively unchanged versus the singly loaded DTX NPs with maximum values of  $3.21 \pm 0.24$  wt% ( $34.21 \pm 0.41\%EE$ ) for C<sub>4</sub>CP,  $3.26 \pm 0.14$  wt% ( $33.86 \pm 0.22\%EE$ ) for C<sub>8</sub>CP, and  $3.29 \pm 0.12$  wt% ( $37.86 \pm 0.49\%EE$ ) for C<sub>10</sub>CP (Table S3).

Next, we examined any differences in dually loaded NP sizes at various CPP %FR (Figure S3). Throughout the C<sub>4</sub>CP and C<sub>8</sub>CP loadings with DTX, the particle size and polydispersity index (PDI) changed very little hovering around 60 nm (0.18–0.25 PDI). However, the

C<sub>10</sub>CP particle size begins to increase from ~85 nm at the lower %FR (< 4%) to ~125 nm at the higher feeding ratios (> 8%), while the PDI stays low between 0.24–0.29. No significant differences in the particle morphology were found between CPPs as their shapes were all spherical (Figure S4).

#### *In vitro* drug release kinetics

We determined the release rates of DTX and CPPs from both the singly and dually loaded PLGA–PEG NPs under physiological sink conditions (Figure 4).<sup>22</sup> All three CPPs displayed limited to no burst release. However, the CPPs exhibited large variations in their release rate for both the singly and dually loaded PLGA–PEG NPs related to their associated fatty acid chain length. For example, the C<sub>4</sub>CP released significantly faster than the C<sub>10</sub>CP in both singly and dually loaded NPs. In both cases, ~50% of the C<sub>4</sub>CP leached to the solvent in the first 4 h and reached complete release within 12 h. In contrast, less than 40% of the encapsulated C<sub>10</sub>CP was released in the first 24 h, and a residual 50–60% remained encapsulated after 48 h. Surprisingly, DTX release also showed a similar dependence on the associated CPP fatty acid length with more rapid

DTX release when incorporated with C<sub>4</sub>CP versus C<sub>10</sub>CP. In general, DTX release from dually loaded NPs occurred faster than the CPPs and was affected to a lesser extent by the CPPs' fatty acid chain length. Due to C<sub>4</sub>CP's low drug loading and rapid release from the NPs we chose to use only the C<sub>8</sub>CP and C<sub>10</sub>CP for *in vitro* and *in vivo* studies.

#### *In vitro* cytotoxicity

The *in vitro* cytotoxicity of the combination NPs was evaluated in aggressive non-small cell (H460) and small cell lung cancer (344SQ) models to determine the combination NPs' therapeutic efficacy (Table S4). Figure 5 compares the half-maximal inhibitory concentration (IC<sub>50</sub>) of free drugs, different molar ratios of co-dosed free drugs, singly loaded NPs, and the dually loaded NPs with both drugs at different molar ratios. The singly C<sub>8</sub>CP loaded NPs produced IC<sub>50</sub> values of 188 ± 20 nM (H460) and 680 ± 72 nM (344SQ), while the singly C<sub>10</sub>CP loaded NPs showed an even greater enhancement with IC<sub>50</sub> values of 78 ± 15 nM (H460) and 150 ± 38 nM (344SQ). Overall, the singly loaded CPP NPs produced IC<sub>50</sub> enhancements ranging from eighteen to eighty-one fold versus free CP. In contrast, loading DTX into NPs showed no enhancement in the drug's cytotoxicity as both its IC<sub>50</sub> values slightly increased to 95 ± 17 nM (H460) and 220 ± 43 nM (344SQ).

Co-encapsulation of CPPs and DTX into a single NP provided even lower IC<sub>50</sub> values. The lowest cumulative drug IC<sub>50</sub> values for dually loaded NPs occurred at loading ratios of 1.2:1 DTX:C<sub>8</sub>CP (26 ± 4 nM = H460, 88 ± 15 nM = 344SQ) and 1.5:1 DTX:C<sub>10</sub>CP (18 ± 4 nM = H460, 70 ± 11 nM = 344SQ). The 1.20:1 DTX:C<sub>8</sub>CP NPs showed a 2.4 (H460) and a 1.7 (344SQ) fold reduction in IC<sub>50</sub> versus both free drugs dosed at the same ratio. Likewise, the 1.5:1 DTX:C<sub>10</sub>CP formulation showed a cytotoxicity enhancement of 2.7 (H460) and 2.2 (344SQ) versus a free drug formulation of the same feeding ratio. However, mixed, singly loaded NPs co-dosed at the same ratio (1.2:1 [DTX NPs + C<sub>8</sub>CP NPs] and 1.5 [DTX NPs + C<sub>10</sub>CP NPs]) did not show a significant difference in cytotoxicity as their dually loaded counterparts. Due to the enhancement of cytotoxicity at these ratios, we chose to use the 1.2:1 DTX:C<sub>8</sub>CP and 1.5:1 DTX:C<sub>10</sub>CP dually loaded NP formulations for further *in vivo* studies.

#### *In vivo* efficacy of NPs in murine lung cancer xenograft

We investigated the *in vivo* treatment efficacy of the loaded NPs in a murine tumor xenograft model using two aggressive lung cancer cell lines (Figure 6). Mice receiving a control injection of PBS (1) showed rapid tumor growth with both tumor models enlarging nearly 20 fold within 12 days. In both tumor models, the combination NP (5) containing C<sub>8</sub>CP and DTX outperformed all other treatment arms by significantly delaying tumor progression the most. Furthermore, the DTX:C<sub>10</sub>CP dually loaded NP (6) outperformed the singly loaded NP combination treatment arms in the 344SQ model (3,4) but gave comparable results to both the free drug combination (2) and mixed C<sub>8</sub>CP NPs + DTX NP arms (3) in the H460 model. Animal survival reciprocated these results with mice receiving the combination NPs showing longer lifespans versus mice given the free drug combo or mixtures of singly loaded NPs (Figure S5).

Our previous work with PLGA-PEG NPs indicated that these particles tend to accumulate within the liver.<sup>24</sup> Furthermore, cisplatin is a known nephrotoxin.<sup>25</sup> Especially with the more potent drug formulations, these concerns could lead to undue toxicity in these off-target organs. Therefore, we investigated the hematological and organ specific toxicity of the new NP formulations. As with other chemotherapies, all mice receiving treatment showed a decrease in white blood cell counts indicating hematological toxicity (Table S5). However, all treatments encouragingly showed low hepato and nephrotoxicity as demonstrated by plasma ALT/AST and BUN/Crea levels, respectively (Table S6), indicating that dosing was well tolerated in these organs. Additionally, animal weight did not fluctuate significantly between treatment arms indicating limited deleterious effects (Figure S6).

## Discussion

The combination of CP and DTX is a proven and effective therapy treatment strategy for a variety of cancer types that may benefit from an NP co-delivery strategy.<sup>5,10–16</sup> Therefore, we sought to evaluate (1) the DTX/CPP combination NPs' properties, and (2) the *in vivo* efficacy of these combination NPs in models of lung cancer.

In combination therapy, the proper dosage and ratio of drugs are required to reach the maximum therapeutic effect.<sup>9</sup> We determined the CPPs and DTX co-loading capacities and ratios in PLGA-PEG NPs (Figures 2, 3, and S2; Tables S1-S3). For both singly and dually loaded NPs, the increased C<sub>10</sub>CP chain length more favorably partitions the CPP within the hydrophobic PLGA core versus its C<sub>4</sub> and C<sub>8</sub> counterparts at %FR greater than 2%. Obviously, this greater C<sub>10</sub>CP loading would allow for higher doses of CP, but this increased loading may not necessarily benefit the combination's efficacy *in vivo* (*vide infra*). Since some combination therapies can affect the loading capacity of one or both drugs within an NP, we analyzed the CPPs' effects on DTX loading and vice versa.<sup>7</sup> As shown in Figure 3 and Tables S2 and S3, both CPPs and DTX did not regulate the loading of the other within the PLGA-PEG NP system. This makes engineering of DTX:CPP combination NPs with a precise drug loading ratio simple, since the %FR of either chemotherapy can be tuned without adversely affecting the other. Therefore, the PLGA-PEG NP provides an ideal system for precision loading of specific CPP and DTX drug ratios.

Previous work within our group has demonstrated that the rate of drug release from an NP carrier can significantly affect therapeutic outcomes making temporally controlled drug release a key consideration in NP design.<sup>22</sup> Since the CPPs' chain length determined the maximum loading capacity, we reasoned that it may also lead to different rates of release from NPs. Unmistakably, a large difference in release rates was noted in both singly and dually loaded NPs (Figure 4). As the aliphatic chain length increases, the CPP release rate dropped. This result correlates nicely with the loading data and, once again, is likely due to C<sub>10</sub>CP's greater proclivity for the hydrophobic PLGA core versus shorter chained derivatives. More surprisingly, DTX release also changed with increased hydrophobicity of the co-encapsulated CPP. We reason the increased hydrophobic environment resulting from the longer decanoic and octanoic acids may interact with the lipophilic DTX aiding in its retention. Regardless, this relationship between chain length and release rate may allow for temporally controlled DTX and CP release engineered to match the requisite pharmacokinetics for effective treatment of a particular disease. Furthermore, the more rapid DTX release before CP delivery correlates nicely with the order the combination is often given in the clinic (DTX → CP).<sup>10,11</sup>

Although previous studies indicate that they are not synergistic, CP and DTX combination therapy displays improved patient outcomes and an additive therapeutic effect against many forms of cancer, particularly for both non-small cell and small cell lung cancers.<sup>10–16,26</sup> This increased efficacy stems mainly from their differing mechanisms of action within the cell that prevents treatment cross resistance. CP promotes apoptosis by forming irreversible DNA cross-links with guanine residues, whereas docetaxel stabilizes the microtubule network thereby blocking mitotic cell division. However, when given in their free form, the two drugs differing physicochemical properties could cause inaccurate and variable exposure of tumors to the necessary drug dosages and ratios leading to a reduction in treatment efficacy and increases in tumor resistance.<sup>27</sup>

Therefore, based on the clinical successes of other NP combination formulations to resolve these challenges, we hypothesized that co-encapsulation within NPs could even further improve the DTX and CPP combination's therapeutic index.<sup>8,27,28</sup> As expected, the combination of both drugs within the same NPs greatly improved the *in vitro* cytotoxicity versus the singly loaded NPs (Figure 5). This large improvement in cytotoxicity confirms that DTX and CPPs are at least additive when given together in NP form.<sup>10–16,29</sup> Furthermore, the PLGA-PEG NPs themselves improved the combination's *in vitro*

activity as evidenced by a greater cytotoxicity than free DTX and CP dosed together at the same ratios. However, singly loaded DTX and CPP NPs given *in combination* at the same ratios produced similar cytotoxicities to the dually loaded NPs. This suggests no advantage to loading both drugs within the same NP at least *in vitro*. However, the primary advantages of co-encapsulation, such as accurate exposure of the target site to a precise drug ratio and modulation of each drugs' release rate, would not fully manifest until evaluated *in vivo* where the advantages of co-encapsulation play a more prominent role.

Indeed, subsequent evaluation of the combination's efficacy *in vivo* showed an advantage to co-encapsulating CPPs and DTX (Figures 6 and S5). The dually loaded DTX:C<sub>8</sub>CP NPs outperformed all other treatment arms by blunting tumor growth the most in both lung cancer models. Even though the aggressive nature of these lung cancer xenograft models caused the tumor growth in all treatment arms to remain high, mice treated with the dually loaded NPs showed a prolonged survival *versus* animals receiving the free drug alone (Figure S5). This significant improvement likely stems from the aforementioned, accurate exposure of the tumor site to both drugs at a specific dose and ratio producing at least an additive therapeutic effect.<sup>10–16</sup> In contrast, the free drug and singly loaded NPs may not equally expose and extravasate both drugs to the site of interest which reduces the therapeutic response. Furthermore, the improved stability and pharmacokinetic profile that NPs impart on their cargo also likely benefited the treatment's efficacy. Despite these increases in combination potency, the off-target liver and kidney toxicity remained low indicating that these treatments were well tolerated.

Interestingly, the choice of CPP used in the formulation also affected the combination's *in vivo* therapeutic index. Despite displaying a similar cytotoxicity to C<sub>8</sub>CP containing NPs *in vitro*, dually and singly loaded formulations of DTX and C<sub>10</sub>CP did not show a significant reduction in tumor growth for the H460 model *versus* free CP and DTX given together. This may be due to the associated release rates of C<sub>8</sub>CP and C<sub>10</sub>CP NP. The *in vitro* release data suggest that the C<sub>10</sub>CP NPs will retain most of its payload after 2 days leaving most of the CP at the tumor periphery.<sup>30</sup> In contrast, the C<sub>8</sub>CP derivative fully released its payload within 2 days allowing for a fuller dosing of the tumor. The difference in the C<sub>10</sub>CP particle size may also play a role in the reduced efficacy. At the %FR used, the C<sub>10</sub>CP particles were nearly twice the diameter of the C<sub>8</sub>CP loaded particles. This may allow preferential extravasation of the C<sub>8</sub>CP NPs into the tumor bed or interior resulting in higher and more even CP and DTX delivery. Regardless, the marked improvement in *in vivo* efficacy for the dually loaded C<sub>8</sub>CP:DTX NPs clearly demonstrates that co-formulation of CP and DTX is therapeutically superior to dosing both drugs in either their free drug form or as singly loaded NPs.

NP delivery vehicles can improve the therapeutic efficacy of drug combinations used in the treatment of cancer by accurately exposing the malignancy to a specific dose and drug ratio. This work demonstrates that the co-delivery of CPPs and DTX from PLGA-PEGNPs improves the combination's *in vivo* efficacy with at least an additive therapeutic effect.<sup>10–16</sup> Furthermore, careful selection of the CPP structure ensured the best therapeutic outcome as demonstrated by the greater tumor volume reduction imparted by C<sub>8</sub>CP *versus* a longer chained C<sub>10</sub>CP derivative. This difference in therapeutic efficacy likely stems from variations in several prominent formulation properties, such as particle size and release kinetics, which are structurally dependent. This work's characterization of these effects will allow for the future engineering and clinical translation of new CPP and DTX NP combinations.

## Appendix A. Supplementary data

Supplementary data to this article can be found online at <http://dx.doi.org/10.1016/j.nano.2016.11.007>.

## References

- Jia J, Zhu F, Ma X, Cao ZW, Li YX, Chen YZ. Mechanisms of drug combinations: interaction and network perspectives. *Nat Rev Drug Discov*. 2009;8:111–28.
- Hu CMJ, Zhang L. Nanoparticle-based combination therapy toward overcoming drug resistance in cancer. *Biochem Pharmacol*. 2012;83:1104–11.
- Lehár J, Krueger AS, Avery W, Heilbut AM, Johansen LM, Price ER, et al. Erratum: synergistic drug combinations tend to improve therapeutically relevant selectivity. *Nat Biotechnol*. 2009;27:864.
- Liao L, Liu J, Dreaden EC, Morton SW, Shopsowitz KE, Hammond PT, et al. A convergent synthetic platform for single-nanoparticle combination cancer therapy: ratiometric loading and controlled release of cisplatin, doxorubicin, and camptothecin. *J Am Chem Soc*. 2014;136:5896–9.
- Kolishetti N, Dhar S, Valencia PM, Lin LQ, Karnik R, Lippard SJ, et al. Engineering of self-assembled nanoparticle platform for precisely controlled combination drug therapy. *Proc Natl Acad Sci U S A*. 2010;107:17939–44.
- Miao L, Guo S, Zhang J, Kim WY, Huang L. Nanoparticles with precise ratiometric co-loading and Co-delivery of gemcitabine monophosphate and cisplatin for treatment of bladder cancer. *Adv Funct Mater*. 2014;24:6601–11.
- Guo S, Lin CM, Xu Z, Miao L, Wang Y, Huang L. Co-delivery of cisplatin and rapamycin for enhanced anticancer therapy through synergistic effects and microenvironment modulation. *ACS Nano*. 2014;8:4996–5009.
- Raut L. Novel formulation of cytarabine and daunorubicin: a new hope in AML treatment. *South Asian J Cancer*. 2015;4:38–40.
- Lancet JE, Cortes JE, Hogge DE, Tallman MS, Kovacsovic TJ, Damon LE, et al. Phase 2 trial of CPX-351, a fixed 5:1 molar ratio of cytarabine/daunorubicin, vs cytarabine/daunorubicin in older adults with untreated AML. *Blood*. 2014;123:3239–46.
- Roth AD, Maibach R, Martinelli G, Fazio N, Aapro MS, Pagani O, et al. Docetaxel (Taxotere®)-cisplatin (TC): an effective drug combination in gastric carcinoma. *Ann Oncol*. 2000;11:301–6.
- Dimopoulos MA, Bakoyannis C, Georgoulas V, Papadimitriou C, Mouloupos LA, Deliveliotis C, et al. Docetaxel and cisplatin combination chemotherapy in advanced carcinoma of the urothelium: a multicenter phase II study of the Hellenic Cooperative Oncology Group. *Ann Oncol*. 1999;10:1385–8.
- Vasey PA, Paul J, Birt A, Junor EJ, Reed NS, Symonds RP, et al. Docetaxel and cisplatin in combination as first-line chemotherapy for advanced epithelial ovarian cancer. Scottish Gynaecological Cancer Trials Group. *J Clin Oncol*. 1999;17:2069–80.
- Park SH, Cho EK, Bang S-M, Shin DB, Lee JH, Lee YD. Docetaxel plus cisplatin is effective for patients with metastatic breast cancer resistant to previous anthracycline treatment: a phase II clinical trial. *BMC Cancer*. 2005;5:21–6.
- Miller VA, Kris MG. Docetaxel (Taxotere) as a single agent and in combination chemotherapy for the treatment of patients with advanced non-small cell lung cancer. *Semin Oncol*. 2000;27:3–10.
- Khuri FR. Docetaxel for locally advanced or metastatic non-small-cell lung cancer. Current data and future directions as front-line therapy. *Oncology (Williston Park)*. 2002;16:53–62.
- Le Chevalier T, Bérille J, Zalberg JR, Millward MJ, Monnier A, Douillard JY, et al. Overview of docetaxel (Taxotere)/cisplatin combination in non-small cell lung cancer. *Semin Oncol*. 1999;26:13–8.
- Park J, Fong PM, Lu J, Russell KS, Booth CJ, Saltzman WM, et al. PEGylated PLGA nanoparticles for the improved delivery of doxorubicin. *Nanomedicine*. 2009;5:410–8.
- Dhar S, Gu FX, Langer R, Farokhzad OC, Lippard SJ. Targeted delivery of cisplatin to prostate cancer cells by aptamer functionalized Pt(IV) prodrug-PLGA-PEG nanoparticles. *Proc Natl Acad Sci U S A*. 2008;105:17356–61.
- Zheng YR, Suntharalingam K, Johnstone TC, Yoo H, Lin W, Brooks JG, et al. Pt(IV) prodrugs designed to bind non-covalently to human serum albumin for drug delivery. *J Am Chem Soc*. 2014;136:8790–8.
- Johnstone TC, Lippard SJ. The effect of ligand lipophilicity on the nanoparticle encapsulation of Pt(IV) prodrugs. *Inorg Chem*. 2013;52:9915–20.
- Danhier F, Ansorena E, Silva JM, Coco R, Le Breton A, Préat V. PLGA-based nanoparticles: an overview of biomedical applications. *J Control Release*. 2012;161:505–22.
- Sethi M, Sukumar R, Karve S, Werner ME, Wang EC, Moore DT, et al. Effect of drug release kinetics on nanoparticle therapeutic efficacy and toxicity. *Nanoscale*. 2014;6:2321–7.
- Hall MD, Dillon CT, Zhang M, Beale P, Cai Z, Lai B, et al. The cellular distribution and oxidation state of platinum(II) and platinum(IV) antitumor complexes in cancer cells. *J Biol Inorg Chem*. 2003;8:726–32.
- Au KM, Min Y, Tian X, Zhang L, Perello V, Caster JM, et al. Improving cancer chemoradiotherapy treatment by dual controlled release of Wortmannin and docetaxel in polymeric nanoparticles. *ACS Nano*. 2015;9:8976–96.
- Miller RP, Tadagavadi RK, Ramesh G, Reeves WB. Mechanisms of cisplatin nephrotoxicity. *Toxins (Basel)*. 2010;2:2490–518.
- Georgoulas V, Aravanis A, Agelidou A, Agelidou M, Chandrinos V, Tsaroucha E, et al. Docetaxel versus docetaxel plus cisplatin as front-line treatment of patients with advanced non-small-cell lung cancer: a randomized, multicenter phase III trial. *J Clin Oncol*. 2004;22:2602–9.
- Ma L, Kohli M, Smith A. Nanoparticles for combination drug therapy. *ACS Nano*. 2013;7:9518–25.
- Humphrey RW, Brockway-Lunardi LM, Bonk DT, Dohoney KM, Doroshov JH, Meech SJ, et al. Opportunities and challenges in the development of experimental drug combinations for cancer. *J Natl Cancer Inst*. 2011;103:1222–6.
- Jamieson ER, Lippard SJ. Structure, recognition, and processing of cisplatin-DNA adducts. *Chem Rev*. 1999;99:2467–98.
- Barua S, Mitragotri S. Challenges associated with penetration of nanoparticles across cell and tissue barriers: a review of current status and future prospects. *Nano Today*. 2014;9:223–43.